Journals of Gerontology: BIOLOGICAL SCIENCES
Cite journal as: J Gerontol A Biol Sci Med Sci 2014 March;69(3):260–269
doi:10.1093/gerona/glt081

Advance Access publication June 22, 2013

Dual Effects of Resveratrol on Arterial Damage Induced By Insulin Resistance in Aged Mice

Stephanie Baron,[1,2] Tatiana Bedarida,[1] Charles-Henry Cottart,[1,3] Francoise Vibert,[1] Emilie Vessieres,[4] Audrey Ayer,[4] Daniel Henrion,[4] Baptiste Hommeril,[5] Jean-Louis Paul,[5,6] Gilles Renault,[7] Bruno Saubamea,[8] Jean-Louis Beaudeux,[1,9] Vincent Procaccio,[4] and Valerie Nivet-Antoine[1,5]

[1]Viva Team—EA 4466, Faculty of Pharmacy, Paris Descartes University, France.
[2]Department of Physiology, Georges Pompidou European Hospital, Assistance publique—Hôpitaux de Paris, France.
[3]Clinical Biochemistry, Pitié-Salpêtrière - Charles Foix Hospital, Assistance publique—Hôpitaux de Paris, France.
[4]CNRS UMR 6214, INSERM U1083, Angers University, France.
[5]Department of Biochemistry, Georges Pompidou European Hospital, Assistance publique—Hôpitaux de Paris, France.
[6]EA 4529, Faculty of Pharmacy, Paris Sud University, Chatenay-Malabry, France.
[7]Institut Cochin, CNRS UMR 8104, and INSERM U1016, Descartes University Sorbonne Paris Cité, France.
[8]Cellular and Molecular Imaging Platform, IFR 71—IMTCE Institute, Faculty of Pharmacy, Paris Descartes University, France.
[9]Clinical Biochemistry, Necker Hospital, Assistance publique—Hôpitaux de Paris, France.

Address corresponding to Stephanie Baron, PharmD, Viva Team—EA 4466, Faculty of Pharmacy, Paris Descartes University, Sorbonne Paris Cité 75006, Paris Cedex, France. Email: stephanie.baron@egp.aphp.fr

Aging leads to increased insulin resistance and arterial dysfunction, with oxidative stress playing an important role. This study explored the metabolic and arterial effects of a chronic treatment with resveratrol, an antioxidant polyphenol compound that has been shown to restore insulin sensitivity and decrease oxidative stress, in old mice with or without a high-protein diet renutrition care. High-protein diet tended to increase insulin resistance and atheromatous risk. Resveratrol improved insulin sensitivity in old mice fed standard diet by decreasing homeostasis model of assessment-insulin resistance and resistin levels. However, resveratrol did not improve insulin resistance status in old mice receiving the high-protein diet. In contrast, resveratrol exhibited deleterious effects by increasing inflammation state and superoxide production and diminishing aortic distensibility. In conclusion, we demonstrate that resveratrol has beneficial or deleterious effects on insulin sensitivity and arterial function, depending on nutritional status in our models.

Key Words: Aging—Resveratrol—Vascular disease—Insulin resistance—Renutrition.

Received December 16, 2012; Accepted May 8, 2013

Decision Editor: Rafael de Cabo, PhD

AGING is characterized by a gradual decline of physiological functions such as glucose homeostasis. Indeed, insulin resistance frequently develops in the elderly and is often associated with protein malnutrition and cardiovascular problems (1). Oxidative stress has been linked to multiple forms of insulin resistance (2,3), especially in the elderly (4–6), and may decrease the effectiveness of renutrition in malnourished elderly patients (3,7). Oxidative stress also plays a central role in arterial dysfunction and vascular aging (8–10). High-protein supply used in renutrition care as recommended by the French health authorities (Haute Autorité de Santé) seems to have a beneficial effect on elderly comorbidities (11). However, detrimental effects of such diets on the vascular system have already been reported, but the effects during elderly renutrition care have never been explored (12).

Resveratrol, a polyphenol found in grapes, has been shown to prevent oxidative stress and inhibit inflammation, probably via NFκB inhibition, and to downregulate proteins at the interface between redox states and glucose metabolism under stressful conditions (8,13–15). Moreover, human clinical trials have shown that resveratrol can restore insulin sensitivity (16–19). Resveratrol treatment may increase NAD+/NADH ratio and/or NAD+ biosynthesis. Resveratrol has been claimed to act upstream of AMPK, which may increase NAD+/NADH ratio and/or NAD+ biosynthesis, and resveratrol has been shown to activate SIRT1 via NAD+ biosynthesis (20–24). Resveratrol may also improve lipid metabolism, reduce the incidence of cardiovascular events, and partially reverse age-related metabolic conditions. However, there are reports that resveratrol activity depends on context, especially diet (25–28).

The hypothesis of our work was that resveratrol would have different effects on old arterial function according to patterns of insulin resistance. To explore this hypothesis, two murine models were proposed: old mice fed a standard diet and old mice fed a high-protein (HP) diet as renutrition care.

The aim of this study was to compare the effect of resveratrol on aging-induced and renutrition-induced insulin resistance and its consequences on the arterial system. Our

study is original because the effects of resveratrol were explored on the molecular stages of endothelial dysfunction (by studying molecular modifications caused by oxidative stress) and on the arterial consequences in terms of reactivity and distensibility (by echo-Doppler analysis).

Methods

Experimental Animals

C57BL/6J male mice (6 and 22 months old) were obtained from Janvier (Le Genest-St-Isle, France) and treated in accordance with the European Parliament and Council Directive 2010/63/EU. They were housed in a temperature- and humidity-controlled room with a 12-h/12-h light–dark cycle and had food and water ad libitum. After 10 days of adaptation, they were randomized into five feeding groups for 12 weeks.

Two diets were provided: a standard diet M20 (SDS), delivering an 18% protein supply as given to adult mice in the animal care unit, or a HP diet (Certificate U8954, Safe), delivering a 31% protein supply that corresponds to renutrition care for elderly mice. These diets were supplemented or not with resveratrol (0.04% w/w). At the beginning of the study, the five groups were set up according to age, diet, and resveratrol treatment: a control group (6-month-old mice) fed a standard diet (n = 20); old mice (22 months) fed a standard diet (OS, n = 21); old mice (22 months) fed a standard diet plus resveratrol (OSR, n = 20); old mice (22 months) fed a HP diet (OD, n = 23); and old mice fed a HP diet plus resveratrol (ODR, n = 22). Food intake was measured daily to assess caloric and resveratrol intakes. This protocol was approved by the local ethics committee (Registration numbers: P2.VNA.060.08, CEEA34.SB.008.12).

At the end of the trial, 12 weeks later, after a 6-hour fasting period (from 6–12 AM), blood samples were taken from tail sections, and glucose levels were measured using a glucometer (One Touch Easy, Life Scan glucometer; One Touch Ultra test strips).

Biochemical Analyses

The vena cava was sectioned from anesthetized mice (5% isofluran inhalation). Blood samples were collected and stored for analyses of serum triglycerides, cholesterol, HDL cholesterol (Architect Ci8200, Abbott), and albumin (green bromocresol method) levels. HDL fractions were measured with a Lipoprint HDL kit (Eurobio) following the manufacturer's instructions. HDL cholesterol was divided into two subfractions: a large HDL cholesterol fraction and a nonlarge HDL cholesterol fraction, corresponding to the sum of small and intermediate HDL cholesterol. A liquid-phase multiplexed technique (Luminex Bioplex, Biorad) was used to determine the systemic parameters. Three kits were used in accordance with the manufacturer's instructions: a Mouse Serum Adipokine-3-plex kit (insulin, resistin, and leptin), a Cytokine/Chemokine kit for KC (Keratinocyte derived Chemokine, CXCL1) and RANTES (Regulated on Activation, Normal T cell Expressed and Secreted, CCL5), and a Gut-Hormone kit for peptide YY (PYY), Lincoplex. An insulin resistance index (homeostasis model of assessment-insulin resistance [HOMA-IR]) was calculated as HOMA-IR = blood glucose level (mmol/L) × insulin (mUI/L)/22.5.

Staining the Aorta With Dihydroethidium

Superoxide production was measured using dihydroethidium, as described previously (29). Briefly, one segment of aorta was fresh frozen in Tissue Tek OCT Compound medium and stored at −80°C. Unfixed frozen sections (10 µm thick) were incubated for 1 hour at 37°C in a humidified chamber with dihydroethidium (10 µM in phosphate-buffered saline). Sections were counterstained with Alexa Fluor 488 Phalloidin (Invitrogen, dilution 1/100) to delimit the artery. Pictures were recorded on a Leica TCS SP2 confocal microscope (excitation wavelength 488 nm, emission wavelengths of 580 and 520 nm for dihydroethidium and phalloidin, respectively). Quantification of superoxide production was carried out using NIH ImageJ software. The intensity of the dihydroethidium stain was measured within the aorta mask and divided by the surface area to obtain fluorescence-density values (arbitrary units/µm^2).

Quantitative Real-Time PCR Analysis

Frozen segments of the liver and aorta were crushed with an Ultra-Turrax J25 instrument (Fisher-Bioblock) for 1 minute in Trizol (Invitrogen). RNA was extracted as described elsewhere (30). An aliquot of 1 µg of total RNA was treated with DNAse I (Invitrogen) and converted into cDNA using Superscript II reverse transcriptase, oligo (dT) $_{12–18}$ primers, and RNAse Out Recombinant Ribonuclease Inhibitor (Invitrogen). cDNA products were subjected to real-time PCR (ABI 7900HT Fast Real-Time PCR). Quantitect SYBR Green PCR and Quantitect primer assay (Qiagen, Courtaboeuf, France) kits were used to quantify TNFα gene expression.

All reactions were carried out in triplicate in a final volume of 20 µL, following the manufacturer's instructions. Ribosomal Protein L4 was used as a housekeeping gene after a validation step to verify equal loading of RNA and cDNA for the reverse transcription and PCR reactions. Data were analyzed using the $2^{-\Delta\Delta Ct}$ method (31).

Hepatic TNFα Western Immunoblot

Liver sample preparations.—Liver fragments were crushed while still frozen, then homogenized in 10 mM phosphate buffer (pH 7.8) containing 1 mM EDTA and protease inhibitor cocktail (1%; Sigma) for 30 seconds, using an Ultra-Turrax homogenizer (Fisher-Bioblock). Homogenates were separated into several aliquots and conserved at −80°C until analysis.

Western immunoblot analysis of liver TNFα.—Samples (40 µg of protein) were loaded onto a sodium dodecyl sulfate–acrylamide gel (15%) and subjected to electrophoresis. Gels were electroblotted to nitrocellulose membrane and probed for TNFα using rabbit anti-mouse TNFα (Abcam; 1/200) and for β-actin using chicken anti-β-actin (Abcam; 1/500), horseradish peroxidase-conjugated anti-rabbit IgG (Sigma; 1/50,000), and anti-chicken IgG (Abcam; 1/4,000) secondary antibodies followed by chemiluminescence detection on the ECL kit using Hyperfilm MP (Amersham). Blots were scanned and their band surface areas analyzed on NIH ImageJ software using the same-sized section of the blot for each scan. The data were expressed as densitometric units relative to β-actin protein.

TNFα Aorta Labeling

Segments of aorta were embedded in Tissue Tek OCT Compound, frozen at −40°C and stored at −80°C. After fixing (paraformaldehyde 4%) and blocking, 20-µm-thick sections were incubated with a primary antibody raised against TNFα (Abcam; 1/100). Labeling was revealed with Alexa Fluor 488 goat anti-rabbit IgG (Invitrogen; 1/200). The endothelium was labeled with rat monoclonal anti-CD31 antibody (BD Pharmingen; 1/100) and revealed with Alexa Fluor 555 goat anti-rat IgG (dilution 1/200). Nuclei were counterstained with To-Pro3 (Invitrogen; 1/500). Negative controls (primary antibodies substituted by nonimmune IgG isotype) did not yield any detectable labeling.

Images were recorded on a Leica TCS SP2 confocal microscope. Endothelial TNFα protein expression was quantified using NIH ImageJ software. Three sections of each aorta were recorded, and four independent sectors of each section were analyzed. TNFα–staining intensities were measured within the endothelium and divided by surface area to give fluorescence-density values (in arbitrary units/µm^2).

Arterial Reactivity Experiments

Aorta and mesenteric artery vasoreactivity experiments were carried out as previously described (32,33). Briefly, a 2-mm-long segment of aorta or second-order mesenteric artery was dissected and mounted on a wire myograph. Two wires were inserted into the lumen of the arteries and fixed to a force transducer and a micrometer, respectively. The arteries were bathed in a 5-mL organ bath containing a physiological salt solution maintained at a pH of 7.4, a pO_2 of 160 mmHg, and a pCO_2 of 37 mmHg. The optimal wall tension was then applied. Artery viability was tested using a potassium-rich solution (80 mmol/L).

A cumulative concentration–response curve to phenylephrine (0.001–10 µmol/L) was then plotted. After a washout, a concentration–response curve for the endothelium-dependent relaxing agent, acetylcholine (0.001–10 µmol/L), was plotted following phenylephrine-induced preconstriction (3 µmol/L). To determine the role played by oxidative stress in the aorta and the reactivity of the mesenteric arteries, the same experiments were then performed after preincubation with catalase (80 U/mL) and tempol (superoxide dismutase analog; 10 µmol/L). The lack of arterial responsiveness to phenylephrine preconstriction revealed arterial aging and left us only a small number of workable mesenteric artery sections (50% could not be used for experiments). The major damage suffered by these arteries also limited the possibility of statistical analyses due to insufficient sample numbers.

Aortic Distensibility

Doppler echography was carried out on anesthetized mice (isofluran inhalation, induced at 3.5%, then maintained with 1.5%) with an Ultrasound Biomicroscope Vevo 770, Visual Sonic, probe 704. Internal and external diameters of the aortas were measured during systole and diastole. Distensibilities were calculated as distensibility = [systole diameter − diastole diameter]/diastole diameter.

Statistical Analyses

One-way ANOVA and Dunn's multiple comparisons test were used for statistical analyses (GraphPad Prism). Results were expressed as means ± *SEM*; statistical significance was set at $p \leq .05$.

Results

Longitudinal Study

OS group mice showed lower caloric intake ($p < .001$; 12.3 ± 0.2 kcal/mouse/d) than controls (13.2 ± 0.2 kcal/mouse/d). OS mice exhibited weight loss during the study, whereas control mice exhibited weight gain (Table 1). There was no significant difference between the OS group and the control group in terms of survival rates at 84 days.

The caloric intake of the OD group was greater than that of OS mice (13.5 ± 0.2 kcal/mouse/d; $p < .001$) though there were no significant differences between their weights. Compared with OS mice, the survival rate of OD mice at 84 days was significantly decreased.

Resveratrol-treated mice (OSR and ODR) ingested approximately 40 mg/kg/d of resveratrol. Compared with their respective untreated matched groups, neither the OSR group nor the ODR group showed any weight modification during the 12 weeks of the study, nor changes in their caloric intake. Resveratrol treatment did not modify survival rates.

Nutritive Parameters

OS mice showed decreased (−15%) serum albumin levels and tended to show increased (+52%) serum PYY levels (Table 1). Serum leptin levels were decreased by 67%. Compared with OS mice, the OD group did not show changes in albuminemia or PYY serum levels although the serum leptin level tended to increase (+13%).

Table 1. Longitudinal Study and Nutritive Parameters

	Control	OS	OD	OSR	ODR
Survival rate at Day 84 (%)	100	95	70$^{\$}$	100	68
Weight (Day 0) (g)	30.3 ± 0.4	31.4 ± 0.4	31.6 ± 0.7	31.9 ± 0.5	30.6 ± 0.8
Weight change at Day 84 (g)	+1.7 ± 0.2	−1.0 ± 0.2***	−1.3 ± 0.7	+0.1 ± 0.3	−1.9 ± 0.9
Serum albumin (g/L)	29.7 ± 0.7	25.2 ± 1.0*	29.0 ± 1.4	27.1 ± 1.0	25.9 ± 0.7
Serum peptide YY (ng/L)	85.5 ± 23.2	130.2 ± 27.2	152.2 ± 34.5	197.1 ± 13.5	215.1 ± 35.2
Serum leptin (ng/L)	2727 ± 466	891 ± 57**	1005 ± 120	1472 ± 193$^{\#}$	415 ± 59$^{\#\#\#}$

Notes: Control group (9-month-old mice fed a standard diet) and groups of aged mice: OS(R), 25-month-old mice fed a standard diet, with or without resveratrol; OD(R), 25-month-old mice fed a high-protein diet, with or without resveratrol. OS mice were compared with control-group mice (*$p < .05$; **$p < .01$; ***$p < .001$); OD mice were compared with OS mice ($^{\$}p < .05$); OSR and ODR mice were compared with OS and OD mice, respectively ($^{\#}p < .05$; $^{\#\#\#}p < .001$). Mean ± *SEM* (Weight and Weight change [g]; Serum albumin [g/L]; Serum peptide YY and Serum leptin [ng/L]); n = 8–23 per group.

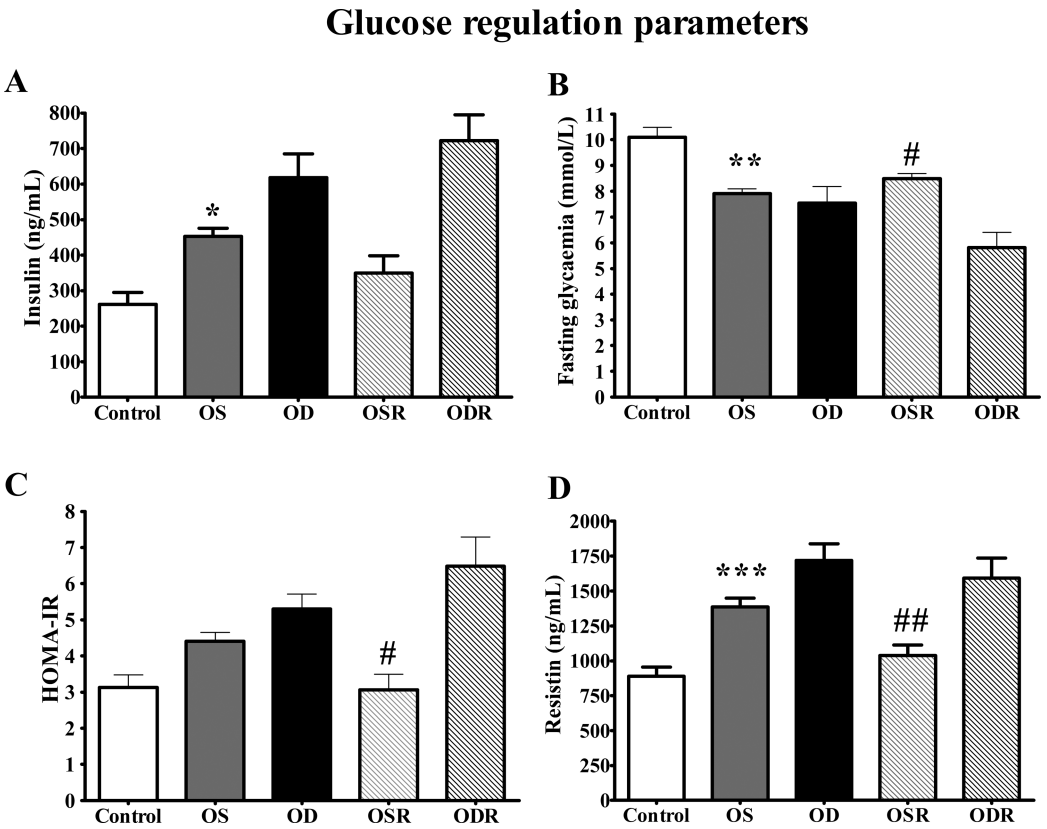

Figure 1. Glucose regulation parameters: **A**, insulinemia; **B**, fasting glycemia; **C**, insulin-resistance index "HOMA-IR"; **D**, resistinemia in the control group (9-month-old mice fed a standard diet) and in old mice (OS(R): 25-month-old mice fed a standard diet, with or without resveratrol; OD(R): 25-month-old mice fed a high-protein diet, with or without resveratrol). OS mice were compared with control mice (*$p < .05$; **$p < .01$; ***$p < .001$); OSR and ODR mice were compared with OS and OD mice, respectively ($^{\#}p < .05$; $^{\#\#}p < .01$). Mean ± *SEM* (insulinemia [ng/mL]; fasting glycemia [mmol/L]; resistinemia [ng/mL]); n = 8–14 per group.

The OSR and ODR groups showed a trend of increasing PYY serum levels, at +65 and +41%, respectively, but no changes in albuminemia. Serum leptin level increased by 65% in OSR mice compared with OS mice, but it decreased by 59% in ODR mice compared with OD mice.

Glucose Regulation Parameters

Compared with the control group, OS mice had increased serum insulin and resistin levels (+73% and +56%, respectively) and increased HOMA-IR (+41%; Figure 1). OS mice had decreased fasting glycemia (−22%) compared with controls. Compared with OS mice, OD mice showed increased insulinemia, HOMA-IR, and resistinemia (+37%, +20%, and +24%, respectively) but no changes in fasting glycemia levels.

Compared with the matched untreated group, OSR mice exhibited a trend toward decreased insulin that resulted in 30% lower HOMA-IR with a 25% lower resistin level, associated with increased fasting glycemia (+8%).

The ODR group showed no significant differences to the OD group in terms of serum insulin, resistin levels, HOMA-IR, or fasting glycemia.

Lipid Metabolism Parameters

OS mice showed decreased levels of triglycerides (−41%), total cholesterol (−21%), and HDL cholesterol (−27%) compared with controls (Figure 2). HDL cholesterol:total cholesterol ratio was decreased by 10% (57.0 ± 1.2% vs 51.5 ± 1.0%, $p < .05$) without any modifications in HDL subfraction partitioning.

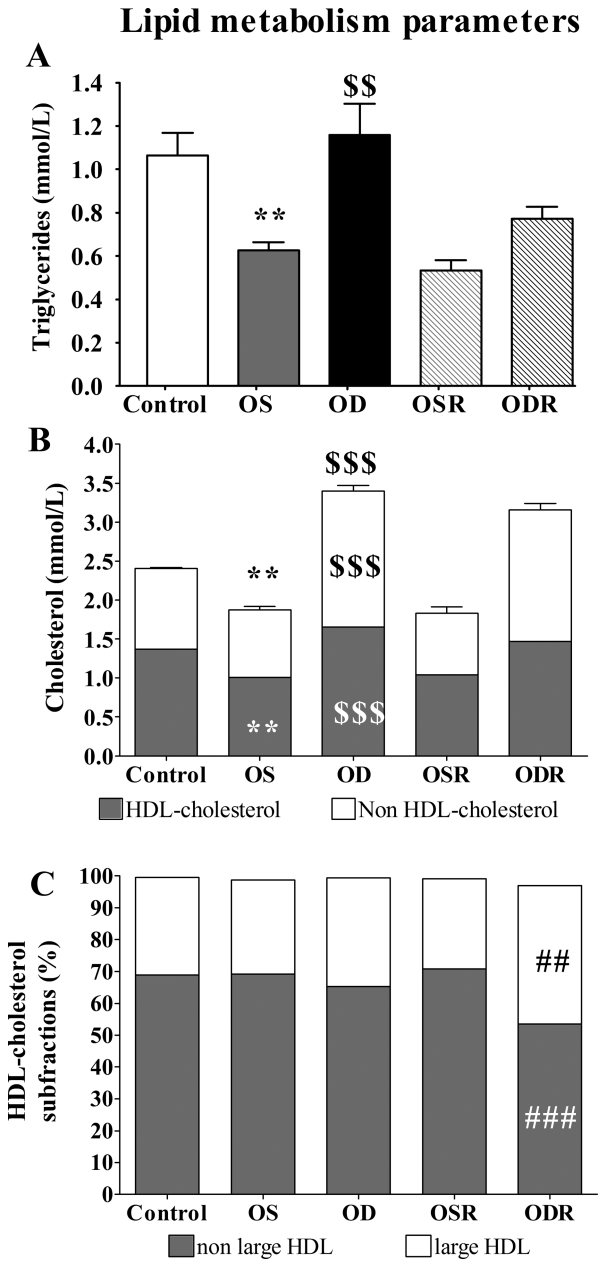

Figure 2. Lipid metabolism parameters: **A**, triglyceridemia; **B**, serum cholesterol level (total cholesterol is the sum of high-density lipoprotein [HDL] cholesterol plus non-HDL cholesterol); **C**, share of each fraction of HDL cholesterol (large and nonlarge HDL cholesterol) in the control group (9-month-old mice fed a standard diet) and in old mice (OS(R): 25-month-old mice fed a standard diet, with or without resveratrol; OD(R): 25-month-old mice fed a high-protein diet, with or without resveratrol). OS mice were compared with control mice ($^{**}p < .01$); OD mice were compared with OS mice ($^{\$\$}p < .01$; $^{\$\$\$}p < .001$); OSR and ODR mice were compared with OS and OD groups, respectively ($^{\#\#}p < .01$; $^{\#\#\#}p < .001$). Mean ± SEM (triglyceridemia and serum cholesterol level [mmol/L]); Percentage (share of each fraction of HDL cholesterol [%]); $n = 8–14$ per group.

The OD group showed higher levels of triglycerides (+85%), total cholesterol (+79%), HDL cholesterol (+65%), and non-HDL cholesterol (+100%) than the OS group. HDL cholesterol:total cholesterol ratio was stable (49.5 ± 0.9%). There was no significant change in HDL subfraction partitioning even though large HDL and nonlarge HDL cholesterol concentrations were increased by +113% and 59%, respectively.

OSR and ODR mice did not show any changes in lipid parameters compared with their matched untreated groups. The only clear difference was that nonlarge HDL fraction decreased significantly (−14%), whereas large HDL fraction increased by 28% in ODR mice compared with the OD group.

Serum KC (CXCL1) and RANTES (CCL5) Levels and Liver TNFα Expression

OS mice showed no significant change in serum KC (CXCL1) or RANTES (CCL5) levels compared with controls, but hepatic TNFα gene expression was increased 2.7-fold (Figure 3). OD mice showed no significant change in serum KC or RANTES levels or hepatic TNFα gene and protein expression compared with OS mice.

OSR mice showed similar serum KC and RANTES levels to the matched non-resveratrol-treated group, whereas ODR mice showed very strongly increased serum KC (+363%) and RANTES (+55%) levels compared with OD mice. Resveratrol treatment had no effect on liver TNFα gene and protein expressions in OSR and ODR mice compared with OS and OD mice, respectively.

Aorta TNFα Expression

Compared with controls, OS mice showed 3.8-fold higher TNFα gene expression in the aorta (Figure 4) and 52% higher TNFα protein expression in the endothelium.

In OD mice, neither aortic TNFα gene expression nor endothelial TNFα protein expression were statistically different from OS.

Neither OSR nor ODR mice showed any differences in TNFα gene or protein expressions in the aorta compared with OS and OD groups, respectively.

Aorta Superoxide Generation

Superoxide production rose by 50% in OS mice compared with controls (Figure 5). Superoxide production in the aortas of OD and OS mice did not significantly vary. Resveratrol treatment had no effect on OSR mice, whereas ODR mice showed 55% higher superoxide production.

Arterial Reactivity

OS mice did not show any significant change in acetylcholine-induced dilation of the aorta, but they did show decreased dilation of the mesenteric arteries ($p < .01$) compared with

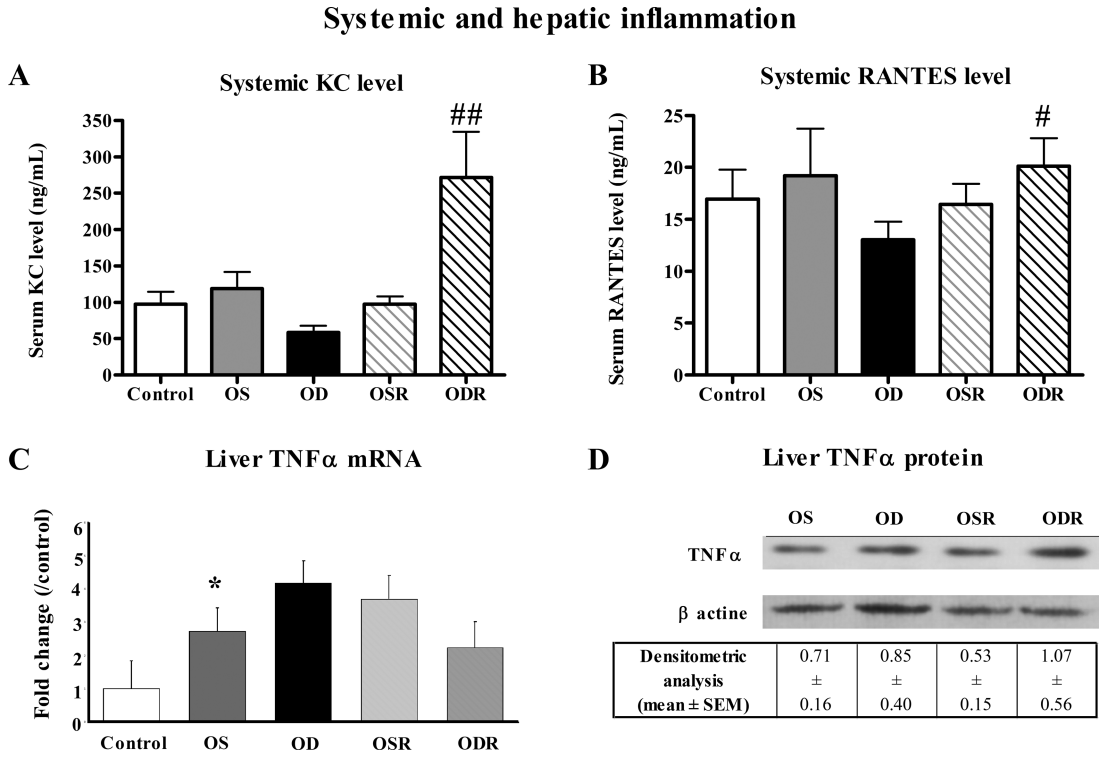

Figure 3. Systemic and hepatic inflammation: **A**, Serum KC level; **B**, Serum RANTES level; **C**, liver TNF alpha mRNA expression (results are represented as fold change compared with the control group); **D**, liver TNF alpha Western Blot; E, Densitometric analysis of Western Blot. Control group (9-month-old mice fed a standard diet); old mice (OS(R): 25-month-old mice fed a standard diet, with or without resveratrol; OD(R): 25-month-old mice fed a high-protein diet, with or without resveratrol). OS mice were compared to control mice (*$p < .05$); OSR and ODR mice were compared with OS and OD mice, respectively ($^{\#}p < .05$; $^{\#\#}p < .01$). Mean ± SEM (Serum KC and RANTES levels [ng/mL]; liver TNF alpha mRNA expression [fold change]; liver TNF alpha Western blot [densitometric arbitrary units]); $n = 6–8$ per group.

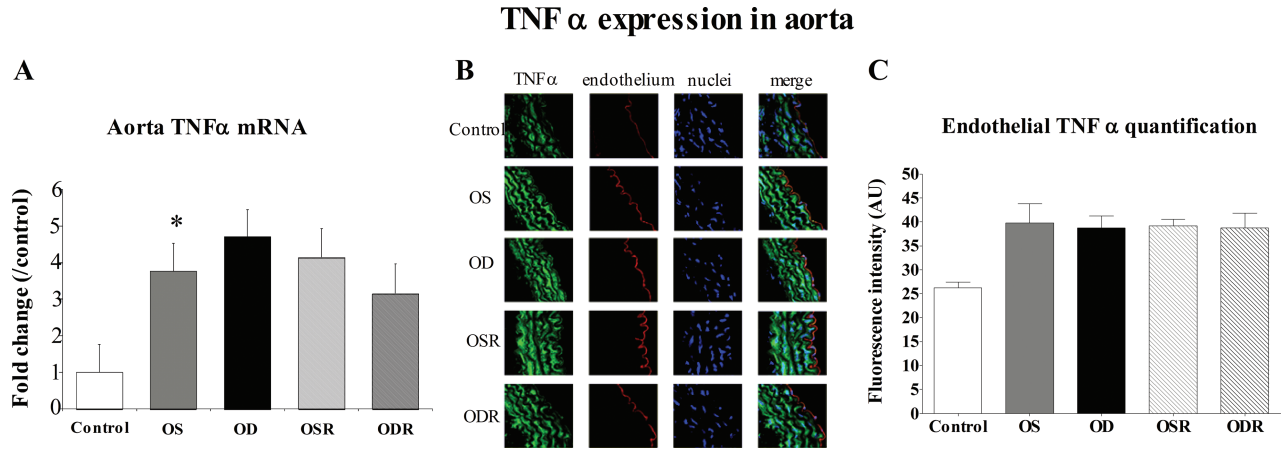

Figure 4. TNF alpha expression in aorta: **A**, aortic TNF alpha mRNA expression (results are represented as fold change compared with the control group); **B**, immunofluorescence in the aorta for TNF alpha (×40); **C**, quantification of TNF alpha protein expression in endothelium, expressed as fluorescence density. All plots represent the control group (9-month-old mice fed a standard diet) and groups with old mice (OS(R): 25-month-old mice fed a standard diet, with or without resveratrol; OD(R): 25-month-old mice fed a highprotein diet, with or without resveratrol). OS mice were compared with control mice (*$p < .05$). Mean ± SEM (aortic TNF alpha mRNA expression [fold change]; quantification of protein expression in endothelium [fluorescence arbitrary units]); $n = 6–8$ per group.

controls group (data not shown). Acetylcholine induced dilation did not significantly change in the aorta or the mesenteric arteries in the OD group compared with OS mice.

Acetylcholine-induced dilation of the aorta and mesenteric arteries was unaffected by resveratrol treatment in OSR and ODR mice. In OD mice, catalase–tempol preincubation did not affect acetylcholine-induced dilation of the aorta or mesenteric arteries (Figures 6A and B).

In the ODR group, catalase–tempol preincubation tended to increase acetylcholine-induced dilation of both the aorta

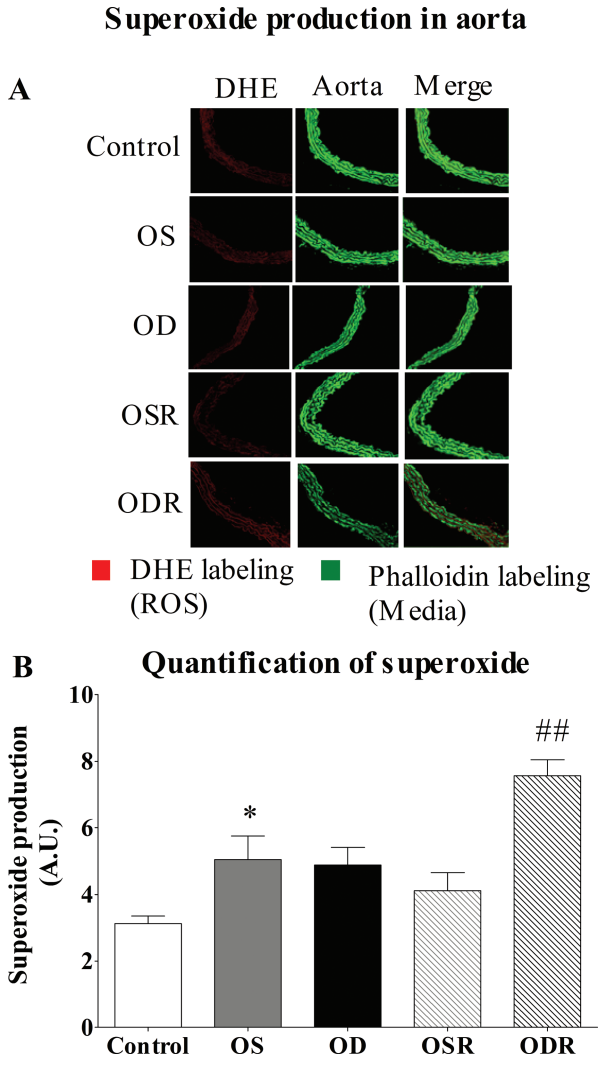

Figure 5. Superoxide production in aorta: **A**, Aorta superoxide generation according to immunofluorescence (dihydroethidium, red) and media (phalloidin, green) labeling (×40). **B**, Quantification of superoxide in the aorta, expressed as fluorescence intensity (A.U.). The plots represent the control group (9-month-old mice fed a standard diet) and groups of old mice (OS(R): 25-month-old mice fed a standard diet, with or without resveratrol; OD(R): 25-month-old mice fed a high-protein diet, with or without resveratrol); OS mice were compared with control mice ($^{*}p < .05$); OSR and ODR mice were compared with the OS and OD mice, respectively ($^{\#\#}p < .01$). Mean ± SEM (quantification of superoxide in the aorta [fluorescence arbitrary units]); n = 4–7 per group.

and mesenteric arteries compared with the nonpreincubated group. Phenylephrine-induced contraction in the aorta tended to increase in the ODR group compared with the OD group (Figure 6C).

Aortic Distensibility

OS mice did not show modified aortic distensibility compared with controls (Figure 6D). Aortic distensibility did not change in OD mice compared with OS mice. Resveratrol treatment had no effect on OSR mice but decreased distensibility in the ODR group.

Discussion

Protein–energy malnutrition affects the great majority of elderly people and is the most prevalent disorder in hospitalized elderly participants (34). This undernutrition state is associated with worse prognosis of associated chronic diseases, including cardiovascular disease that is the main cause of death in this elderly population (34,35).

Renutrition could improve morbidity and mortality in old age (36), but it proves difficult to achieve in elderly patients (37). One possible explanation is that renutrition could depend on the degree of insulin resistance, which is closely related to oxidative stress (3,10) and has already been incriminated in endothelial cell dysfunction (38,39) and vascular aging (9).

Resveratrol, a well-known antioxidant and anti-inflammatory molecule, has been shown to improve insulin sensitivity. This molecule could be a good candidate for slowing down the impairment of glucose tolerance and vascular aging, and a combination resveratrol with a renutrition strategy could have potential benefits for elderly patients.

Renutrition Care Increases Insulin Resistance, Disrupts Lipid Metabolism, and Raises Liver and Aorta Inflammation

Our aged mice (OS group) exhibited a malnutrition state characteristic of aged people, as shown by their reduced weight, hypoalbuminemia, and decreased cholesterol and leptin levels (7,40). In addition, lower triglyceride concentrations and a tendency toward increased PYY levels have been observed, as commonly seen in aged people with anorexia (41).

Focusing on glucose metabolism, hyperinsulinemia and HOMA-IR reflected a serious insulin-resistant state, which was confirmed by increased resistin levels. OS mice showed low fasting glycemia, which could be the consequence of low glucose production, especially due to insufficient gluconeogenesis (42). This may be due to the NAD+-pool depletion observed in the elderly, as reported in recent studies (43,44). The aortic oxidative stress and inflammation observed in OS mice (TNFα expression increased not only in the endothelium but also in whole aorta by 62%; data not shown), has been shown to be related to an insulin-resistant state (45).

To fight against malnutrition in human patients, the French institution "Haute Autorité de Santé" recommends restoring caloric intake with a protein supply (11). The HP diet used in this study restored caloric intake. However, the renutrition process can be lengthy, and success is tightly related to the patient's age (37). In this study, the renutrition process tended to restore serum leptin and albumin levels in elderly mice (11,35). However, this HP diet is also known to induce insulin resistance (46). The trend toward increased insulin and the significantly increased serum IGF-I levels (OD 378 ± 13 pg/mL vs OS 283 ± 27 pg/mL, +34%, $p < .05$)

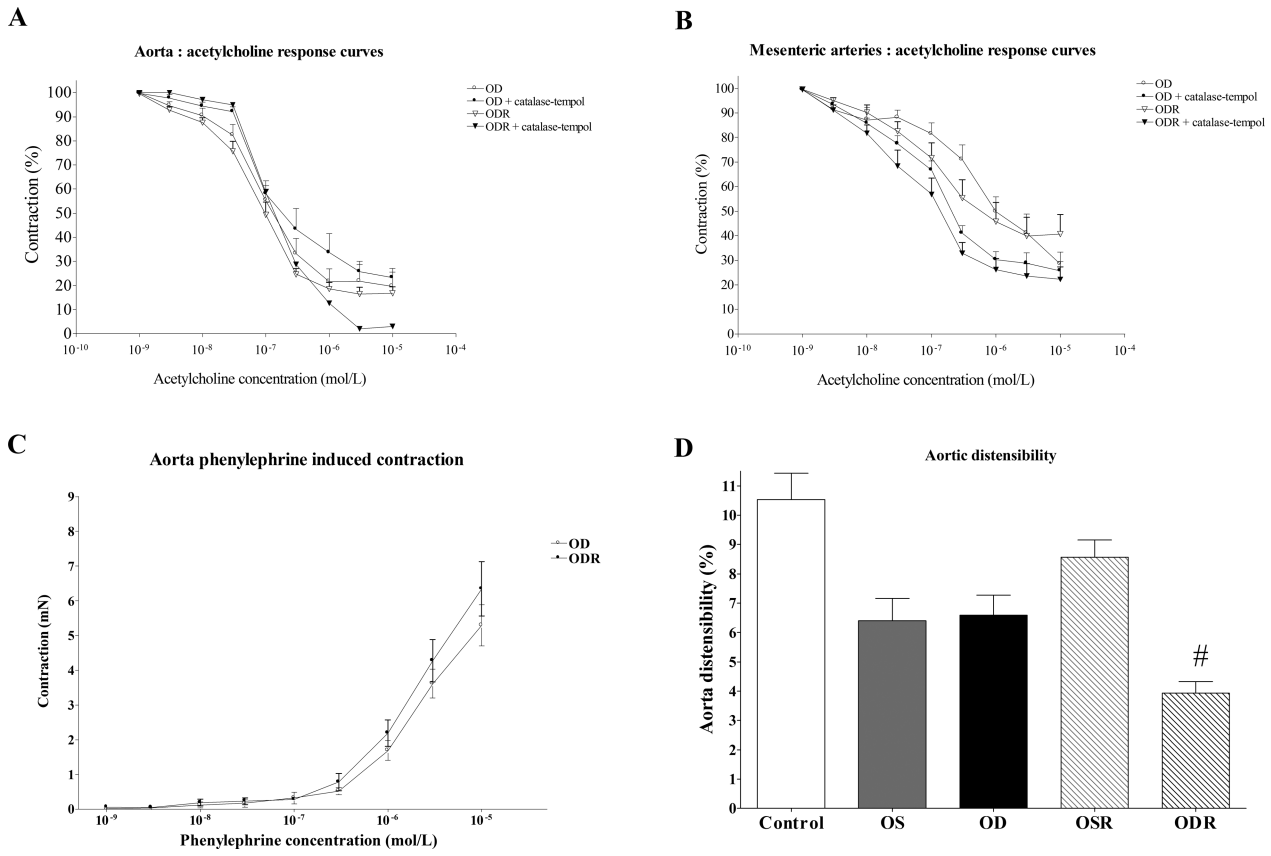

Figure 6. **A** and **B**, Effect of catalase-tempol preincubation on acetylcholine-induced dilation of the aorta (**A**) and mesenteric arteries (**B**) isolated from OD and ODR mice (n = 6–8 per group). Data are expressed as percentages of contraction; **C**, Aortic phenylephrine-induced contraction in OD and ODR groups (n = 6–8 per group); **D**, Aortic distensibility (n = 8–11 per group). All plots represent the control group (9-month-old mice fed a standard diet) and groups of old mice (OS(R): 25-month-old mice fed a standard diet, with or without resveratrol; OD(R): 25-month-old mice fed a high-protein diet, with or without resveratrol). OSR and ODR mice were compared with OS and OD mice, respectively ($^{\#}p < .05$). Mean ± *SEM* (aorta and mesenteric arteries acetylcholine responses curves [% contraction]; aortic phenylephrine-induced contraction [%]; aortic distensibility [%]).

observed in OD mice is in accordance with the presence of an insulin resistance state and with Baur's observations made under another high-calorie diet (47). This insulin resistance associated with high triglyceride levels might be the consequence of increased free fatty acid levels, as described previously (48,49), especially in a context of low glucose supply (12). We did observe increased total cholesterol and non-HDL cholesterol levels. Large HDL fractions are enriched with apolipoprotein E and bind to LDL receptors with high affinity; large HDL fractions are the major class of plasma lipoproteins that deliver lipids to peripheral tissues (50). Thus, the rise of this HDL fraction may increase atheromatous risk under this type of HP diet, as suggested by Foo (12). Moreover, HDL cholesterol:total cholesterol ratio was reduced, which may be predictive of increased susceptibility to atherogenesis (51). These metabolic disorders are associated with increased oxidative stress and inflammation of the aorta induced by aging. They could have vascular and potent cardiovascular consequences that could be responsible for the increased mortality observed in our OD model.

Resveratrol Does not Improve Insulin Resistance and Predicts an Increased Susceptibility to Atherogenesis, Increased Oxidative Stress in the Aorta, and Diminished Aortic Distensibility in OD Mice

The benefits of resveratrol to reduce insulin resistance have been investigated in several studies (19,52,53). The resveratrol dose administered *per os* in this study was around 40 mg/kg/d for 3 months. Depending on authors, this dose would correspond to the dose used in numerous clinical studies (19,47,54) or to a lower daily dose in humans (18,55).

Our results show that resveratrol improved glucose metabolism in the OSR group. The reduction in insulin resistance in OSR mice receiving resveratrol is highlighted by the decreased HOMA-IR and resistin levels. Interestingly, these results corroborated a recent study by Crandall JP in humans, which reported that resveratrol improves insulin sensitivity and postmeal plasma glucose in old participants with age-related glucose intolerance (19). These effects of resveratrol could be the result of an increase in NAD+ levels, as reported by Park (28). In a previous study, we

had shown that resveratrol changes NAD+/NADH balance toward increasing NAD+ concentration in the liver mitochondria of these OSR mice (personal data, V Procaccio). An increase of NAD+ level enhances substrate supply to the respiratory chain by both the tricarboxylic-acid cycle and fatty-acid oxidation, hence providing more energy. The resveratrol-induced improvement of mitochondrial function and glucose tolerance could involve AMPK and/or sirtuin (20–24). In our study, resveratrol seemed to be beneficial to the malnourished state of physiological aging (OS model). By restoring insulin sensitivity, it helped maintain body weight and restore leptin levels.

Conversely, in mice fed the HP diet (ODR mice), resveratrol failed to change fasting glycemia, HOMA-IR, resistin levels, or IGF-I level, and the HP diet seemed to reduce the beneficial effects of resveratrol on insulin resistance. In ODR mice, resveratrol led to a decrease in triglyceride and leptin serum levels, in agreement with Timmers et al.'s results in humans (18). Some studies have shown that resveratrol modulates the regulation of genes related to lipid metabolism, which in the context of an atherogenic diet leads to increased lipolysis and decreased lipogenesis (23). This increased lipolysis could be responsible for the NFκB pathway activation that leads to systemic inflammation (48). ODR mice showed an inflammatory state, with increased serum KC and RANTES levels. KC, through endothelial release, has been already shown to promote atherosclerosis (56). Moreover, resveratrol supplementation increased systemic RANTES levels in ODR mice, suggesting a possible increase in monocyte adherence to endothelial cells. Resveratrol supplementation increased reactive oxygen species in ODR mice arteries, evidencing a deleterious effect of resveratrol on oxidative stress and inflammation. These data do not confirm those found in other studies (13,14,57). However, the effects of resveratrol in these studies were observed on a model of acute and pharmacologically induced inflammation and oxidative stress, whereas, in our model, the systemic low-grade inflammation induced by HP diet was not detectable. Even though total and non-HDL concentrations of cholesterol were unchanged, the HDL cholesterol fraction and the HDL cholesterol:total cholesterol ratio tended to decrease in ODR mice, thus possibly increasing atherosclerosis risk factors (51). Moreover, regarding the HDL subfractions in ODR mice, resveratrol was responsible for a shift in HDL fractions from nonlarge to larger fractions of cholesterol. Furthermore, resveratrol also tended to increase aorta phenylephrine contraction and worsened the diminishing aorta distensibility induced by aging in OD mice. Taken together, these results strongly suggest that resveratrol, when associated with HP diet in old mice, may increase the risk factors associated with atherogenesis by triggering vascular alterations and could represent an additional risk factor for the cardiovascular system when added to a HP diet.

Conclusion

Taken together, our data show that resveratrol could reduce insulin resistance in old age. However, our study also highlights that in a HP diet context, not only are the beneficial effects of resveratrol abrogated but, more importantly, resveratrol supplementation could have deleterious effects on arterial function.

Funding

This work was supported by funds from the French Ministry of Research and Technology under a 4-year contract (EA 4466, 2010–2013).

Acknowledgments

We thank the animal facilities (Paris Descartes University) for animal care, the company Yvery for the supplying the resveratrol, the Cellular and Molecular Imaging platform of the IFR 71-IMTCE Institute, and Prof. A. Jardel, Dr. J-L. Golmard and Dr. C. Boulanger for their valuable advice.

Conflict of Interest

The authors have no conflicts of interest to declare.

References

1. Verhagen SN, Wassink AM, van der Graaf Y, Gorter PM, Visseren FL; SMART Study Group. Insulin resistance increases the occurrence of new cardiovascular events in patients with manifest arterial disease without known diabetes. the SMART study. *Cardiovasc Diabetol*. 2011;10:100.
2. Houstis N, Rosen ED, Lander ES. Reactive oxygen species have a causal role in multiple forms of insulin resistance. *Nature*. 2006;440:944–948.
3. Hebert-Schuster M, Fabre EE, Nivet-Antoine V. Catalase polymorphisms and metabolic diseases. *Curr Opin Clin Nutr Metab Care*. 2012;15:397–402.
4. Abel ED, O'Shea KM, Ramasamy R. Insulin resistance: metabolic mechanisms and consequences in the heart. *Arterioscler Thromb Vasc Biol*. 2012;32:2068–2076.
5. Hasegawa Y, Saito T, Ogihara T, et al. Blockade of the nuclear factor-κB pathway in the endothelium prevents insulin resistance and prolongs life spans. *Circulation*. 2012;125:1122–1133.
6. Hebert-Schuster M, Cottart CH, Laguillier-Morizot C, et al. Catalase rs769214 SNP in elderly malnutrition and during renutrition: is glucagon to blame? *Free Radic Biol Med*. 2011;51:1583–1588.
7. Fabre EE, Raynaud-Simon A, Golmard JL, et al. Gene polymorphisms of oxidative stress enzymes: prediction of elderly renutrition. *Am J Clin Nutr*. 2008;87:1504–1512.
8. Ungvari Z, Kaley G, de Cabo R, Sonntag WE, Csiszar A. Mechanisms of vascular aging: new perspectives. *J Gerontol A Biol Sci Med Sci*. 2010;65:1028–1041.
9. Collins AR, Lyon CJ, Xia X, et al. Age-accelerated atherosclerosis correlates with failure to upregulate antioxidant genes. *Circ Res*. 2009;104:e42–e54.
10. Nivet-Antoine V, Labat C, El Shamieh S, et al. Relationship between catalase haplotype and arterial aging. *Atherosclerosis*. 2013;227:100–105.
11. HAS (Haute Autorité de Santé). *Clinical Practice Guidelines. Nutritional Support Strategy for Protein-Energy Malnutrition in the Elderly*. Saint-Denis, France: HAS; 2007.
12. Foo SY, Heller ER, Wykrzykowska J, et al. Vascular effects of a low-carbohydrate high-protein diet. *Proc Natl Acad Sci U S A*. 2009;106:15418–15423.
13. Hassan-Khabbar S, Cottart CH, Wendum D, et al. Postischemic treatment by trans-resveratrol in rat liver ischemia-reperfusion: a possible strategy in liver surgery. *Liver Transpl*. 2008;14:451–459.

14. Hassan-Khabbar S, Vamy M, Cottart CH, et al. Protective effect of post-ischemic treatment with trans-resveratrol on cytokine production and neutrophil recruitment by rat liver. *Biochimie*. 2010;92:405–410.
15. Nivet-Antoine V, Cottart CH, Lemaréchal H, et al. trans-Resveratrol downregulates Txnip overexpression occurring during liver ischemia-reperfusion. *Biochimie*. 2010;92:1766–1771.
16. Brasnyó P, Molnár GA, Mohás M, et al. Resveratrol improves insulin sensitivity, reduces oxidative stress and activates the Akt pathway in type 2 diabetic patients. *Br J Nutr*. 2011;106:383–389.
17. Cottart CH, Nivet-Antoine V, Beaudeux JL. A review of recent data on the metabolism, biological effects and toxicity of resveratrol in humans. *Mol Nutr Food Res*. 2013. doi:10.1002/mnfr.201200589. In press.
18. Timmers S, Konings E, Bilet L, et al. Calorie restriction-like effects of 30 days of resveratrol supplementation on energy metabolism and metabolic profile in obese humans. *Cell Metab*. 2011;14:612–622.
19. Crandall JP, Oram V, Trandafirescu G, et al. Pilot study of resveratrol in older adults with impaired glucose tolerance. *J Gerontol A Biol Sci Med Sci*. 2012;67:1307–1312.
20. Cantó C, Gerhart-Hines Z, Feige JN, et al. AMPK regulates energy expenditure by modulating NAD+ metabolism and SIRT1 activity. *Nature*. 2009;458:1056–1060.
21. Chung JH, Manganiello V, Dyck JR. Resveratrol as a calorie restriction mimetic: therapeutic implications. *Trends Cell Biol*. 2012;22:546–554.
22. Baur JA, Ungvari Z, Minor RK, Le Couteur DG, de Cabo R. Are sirtuins viable targets for improving healthspan and lifespan? *Nat Rev Drug Discov*. 2012;11:443–461.
23. Price NL, Gomes AP, Ling AJ, et al. SIRT1 is required for AMPK activation and the beneficial effects of resveratrol on mitochondrial function. *Cell Metab*. 2012;15:675–690.
24. Feige JN, Lagouge M, Canto C, et al. Specific SIRT1 activation mimics low energy levels and protects against diet-induced metabolic disorders by enhancing fat oxidation. *Cell Metab*. 2008;8:347–358.
25. Do GM, Kwon EY, Kim HJ, et al. Long-term effects of resveratrol supplementation on suppression of atherogenic lesion formation and cholesterol synthesis in apo E-deficient mice. *Biochem Biophys Res Commun*. 2008;374:55–59.
26. Baur JA, Sinclair DA. Therapeutic potential of resveratrol: the in vivo evidence. *Nat Rev Drug Discov*. 2006;5:493–506.
27. Wang C, Wheeler CT, Alberico T, et al. The effect of resveratrol on lifespan depends on both gender and dietary nutrient composition in Drosophila melanogaster. *Age (Dordr)*. 2013;35:69–81.
28. Park SJ, Ahmad F, Philp A, et al. Resveratrol ameliorates aging-related metabolic phenotypes by inhibiting cAMP phosphodiesterases. *Cell*. 2012;148:421–433.
29. Nijmeh J, Moldobaeva A, Wagner EM. Role of ROS in ischemia-induced lung angiogenesis. *Am J Physiol Lung Cell Mol Physiol*. 2010;299:L535–L541.
30. Chomczynski P, Sacchi N. Single-step method of RNA isolation by acid guanidinium thiocyanate-phenol-chloroform extraction. *Anal Biochem*. 1987;162:156–159.
31. Livak KJ, Schmittgen TD. Analysis of relative gene expression data using real-time quantitative PCR and the 2(-Delta Delta C(T)) Method. *Methods*. 2001;25:402–408.
32. Loufrani L, Dubroca C, You D, et al. Absence of dystrophin in mice reduces NO-dependent vascular function and vascular density: total recovery after a treatment with the aminoglycoside gentamicin. *Arterioscler Thromb Vasc Biol*. 2004;24:671–676.
33. Mulvany MJ, Halpern W. Contractile properties of small arterial resistance vessels in spontaneously hypertensive and normotensive rats. *Circ Res*. 1977;41:19–26.
34. Bouillanne O, Morineau G, Dupont C, et al. Geriatric Nutritional Risk Index: a new index for evaluating at-risk elderly medical patients. *Am J Clin Nutr*. 2005;82:777–783.
35. Nivet-Antoine V, Golmard JL, Coussieu C, Piette F, Cynober L, Bouillanne O. Leptin is better than any other biological parameter for monitoring the efficacy of renutrition in hospitalized malnourished elderly patients. *Clin Endocrinol (Oxf)*. 2011;75:315–320.
36. Newman AB, Yanez D, Harris T, Duxbury A, Enright PL, Fried LP; Cardiovascular Study Research Group. Weight change in old age and its association with mortality. *J Am Geriatr Soc*. 2001;49:1309–1318.
37. Walrand S, Chambon-Savanovitch C, Felgines C, et al. Aging: a barrier to renutrition? Nutritional and immunologic evidence in rats. *Am J Clin Nutr*. 2000;72:816–824.
38. Suvorava T, Lauer N, Kumpf S, Jacob R, Meyer W, Kojda G. Endogenous vascular hydrogen peroxide regulates arteriolar tension in vivo. *Circulation*. 2005;112:2487–2495.
39. Suvorava T, Kojda G. Reactive oxygen species as cardiovascular mediators: lessons from endothelial-specific protein overexpression mouse models. *Biochim Biophys Acta*. 2009;1787:802–810.
40. Bouillanne O, Golmard JL, Coussieu C, et al. Leptin a new biological marker for evaluating malnutrition in elderly patients. *Eur J Clin Nutr*. 2007;61:647–654.
41. Di Francesco V, Fantin F, Omizzolo F, et al. The anorexia of aging. *Dig Dis*. 2007;25:129–137.
42. Atherton HJ, Gulston MK, Bailey NJ, et al. Metabolomics of the interaction between PPAR-alpha and age in the PPAR-alpha-null mouse. *Mol Syst Biol*. 2009;5:259.
43. Braidy N, Guillemin GJ, Mansour H, Chan-Ling T, Poljak A, Grant R. Age related changes in NAD+ metabolism oxidative stress and Sirt1 activity in wistar rats. *PLoS One*. 2011;6:e19194.
44. Massudi H, Grant R, Braidy N, Guest J, Farnsworth B, Guillemin GJ. Age-associated changes in oxidative stress and NAD+ metabolism in human tissue. *PLoS One*. 2012;7:e42357.
45. Evans JL, Goldfine ID, Maddux BA, Grodsky GM. Are oxidative stress-activated signaling pathways mediators of insulin resistance and beta-cell dysfunction? *Diabetes*. 2003;52:1–8.
46. Burcelin R, Crivelli V, Dacosta A, Roy-Tirelli A, Thorens B. Heterogeneous metabolic adaptation of C57BL/6J mice to high-fat diet. *Am J Physiol Endocrinol Metab*. 2002;282:E834–E842.
47. Baur JA, Pearson KJ, Price NL, et al. Resveratrol improves health and survival of mice on a high-calorie diet. *Nature*. 2006;444:337–342.
48. Tripathy D, Mohanty P, Dhindsa S, et al. Elevation of free fatty acids induces inflammation and impairs vascular reactivity in healthy subjects. *Diabetes*. 2003;52:2882–2887.
49. Steinberg HO, Paradisi G, Hook G, Crowder K, Cronin J, Baron AD. Free fatty acid elevation impairs insulin-mediated vasodilation and nitric oxide production. *Diabetes*. 2000;49:1231–1238.
50. de Silva HV, Más-Oliva J, Taylor JM, Mahley RW. Identification of apolipoprotein B-100 low density lipoproteins, apolipoprotein B-48 remnants, and apolipoprotein E-rich high density lipoproteins in the mouse. *J Lipid Res*. 1994;35:1297–1310.
51. LeBoeuf RC, Tsao WW, KIirk E, Childs MT. Cholesterol feeding induces cholesterol-rich VLDL in atherosclerosis-susceptible mice regardless of dietary fat content. *Nutr Res*. 1993;13:549–561.
52. Pearson KJ, Baur JA, Lewis KN, et al. Resveratrol delays age-related deterioration and mimics transcriptional aspects of dietary restriction without extending life span. *Cell Metab*. 2008;8:157–168.
53. Barger JL, Kayo T, Vann JM, et al. A low dose of dietary resveratrol partially mimics caloric restriction and retards aging parameters in mice. *PLoS One*. 2008;3:e2264.
54. Lagouge M, Argmann C, Gerhart-Hines Z, et al. Resveratrol improves mitochondrial function and protects against metabolic disease by activating SIRT1 and PGC-1alpha. *Cell*. 2006;127:1109–1122.
55. Reagan-Shaw S, Nihal M, Ahmad N. Dose translation from animal to human studies revisited. *FASEB J*. 2008;22:659–661.
56. Zhou Z, Subramanian P, Sevilmis G, et al. Lipoprotein-derived lysophosphatidic acid promotes atherosclerosis by releasing CXCL1 from the endothelium. *Cell Metab*. 2011;13:592–600.
57. Abraham J, Johnson RW. Consuming a diet supplemented with resveratrol reduced infection-related neuroinflammation and deficits in working memory in aged mice. *Rejuvenation Res*. 2009;12:445–453.